

# CMTM6 and PD-L1 are independent prognostic biomarkers in head and neck squamous cell carcinoma

**Anne-Sophie Becker**

Rostock University Medical Center

**Sarah Zonnur**

Rostock University Medical Center

**Annette Zimpfer**

Rostock University Medical Center

**Mareike Krause**

Rostock University Medical Center

**Björn Schneider**

Rostock University Medical Center

**Daniel Fabian Strueder**

Rostock University Medical Center

**Ann-Sophie Burmeister**

Rostock University Medical Center

**Andreas Erbersdobler**

Rostock University Medical Center

**Christian Junghanss**

Rostock University Medical Center

**Claudia Maletzki** (✉ [claudia.maletzki@med.uni-rostock.de](mailto:claudia.maletzki@med.uni-rostock.de))

Rostock University Medical Center

---

## Research Article

### Keywords:

**Posted Date:** October 3rd, 2022

**DOI:** <https://doi.org/10.21203/rs.3.rs-2111803/v1>

**License:**   This work is licensed under a Creative Commons Attribution 4.0 International License.

[Read Full License](#)

# Abstract

The predictive potential of immunological markers are not fully understood in head and neck squamous cell carcinomas (HNSCC). We retrospectively analyzed 129 treatment-naive HNSCCs for programmed death ligand 1 (PD-L1) and CKLF-like MARVEL transmembrane domain-containing 6 (CMTM6) expression, tumor-infiltrating leukocytes (TILs), and tumor-associated macrophages (TAMs). We evaluated mutual relationships among these markers, HPV-status, and overall survival (OS). PD-L1 and CMTM6 expression (combined positive score  $\geq 1$  and  $\geq 5$ ) was detected in  $\sim 75\%$  of HNSCCs. The HPV-status had a minor impact on expression of either marker. Nearly all PD-L1-positive cases showed simultaneous CMTM6 expression in comparable staining patterns. Tumors with PD-L1 ( $p < 0.0001$ ) and/or CMTM6 ( $p < 0.05$ ) expression showed the best OS. A high density of TILs ( $p < 0.01$ ), CD8<sup>+</sup> T cells ( $p < 0.001$ ), and a CD68/CD163 ratio  $> 1$  had prognostic relevance. PD-L1 and CMTM6 correlated with density of TILs and CD8<sup>+</sup> cells (Spearman  $r =$  range from 0.22 to 0.34), but not with HPV-status.

Our results identify CMTM6 as an important interaction partner in the crosstalk between TILs, CD8<sup>+</sup> T cells, and PD-L1, mediating anticancer efficacies. CMTM6 evaluation may be helpful for prognostic prediction and additionally serve as a reliable biomarker for selecting HNSCC patients eligible for ICIs treatment.

## Introduction

Head and neck squamous cell carcinoma (HNSCC) is the eighth most common malignancy worldwide. HNSCC develop often because of chronic alcohol and tobacco use, or an oncogenic human papillomavirus (HPV) infection [1, 2]. Accordingly, these tumors are categorized into HPV<sup>pos</sup> or HPV<sup>neg</sup>, with each subtype showing different anatomical locations, molecular signatures, and clinical presentations [3, 4]. This heterogeneity and the fact that patients are often diagnosed at a locally advanced or metastatic disease stage, is challenging for conventional treatment approaches, such as surgery or chemo-radiotherapy. Immune-checkpoint inhibitors (ICIs) represent a cutting-edge new treatment in HNSCC. However, early studies yielded a mixed response, with only 20% of patients benefitting from ICIs [5–7].

The stromal composition and the tumor microenvironment (TME), including numbers of CD8<sup>+</sup> T cells, an IFN- $\gamma$  signature, a high tumor mutational burden, and PD-L1 expression levels, are prognostic for treatment response and outcome [8, 9]. In HNSCC, the TME is composed of tumor-infiltrating immune cells, such as CD4<sup>+</sup> and CD8<sup>+</sup> T cells, myeloid-derived suppressor cells, and tumor-associated M1- or M2-polarized macrophages (TAMs) that interact with tumor cells to promote or suppress growth [10]. PD-L1 is found on both tumor and tumor-infiltrating immune cells and can be used as a biomarker to select for patients eligible to immunotherapy. In most cases, PD-L1 abundance is calculated by applying the combined positive score (CPS), with expression  $\geq 1$  considered positive [11, 12]. In HNSCC, confounding factors such as intratumor heterogeneity may impair validity [13]. Accordingly, the predictive value of the PD-L1-CPS is moderate and objective responses towards PD1 blockade are sometimes regardless of the

PD-L1 status [14, 15]. Hence, PD-L1 alone is not sufficient to predict patients' outcome and additional reliable markers are necessary.

A very interesting candidate is the CKLF-like MARVEL transmembrane domain-containing 6 (CMTM6) [16]. CMTM6 stabilizes PD-L1 *via* physical interaction and co-localization at the cell surface and triggers CD163<sup>+</sup> M2-like macrophage polarization [17]. Depending on the tumor location, CMTM6 is either associated with improved or worse treatment response and outcome [18, 19]. Another recently identified function of CMTM6 is the induction of chemoresistance, especially towards Cisplatin via activation of the *Wnt* signaling [20]. Hence, CMTM6 is an emerging target in refractory HNSCC – especially those selected for 2nd line immunotherapy. Before implementing CMTM6 in pathological routine diagnostic, a deeper understanding on its spatial distribution and its prognostic value is imperative.

In this study, we examined the expression pattern of CMTM6 and different immune-related biomarkers in treatment-naïve advanced HNSCCs from different anatomical sites. We additionally correlated our findings with the expression levels of PD-L1 and the immune cell infiltration pattern within tumors. Our study identified CMTM6 as a critical factor for survival of HPV<sup>pos</sup> and HPV<sup>neg</sup> HNSCCs, that should be actively involved in therapy decision.

## Material And Methods

### Patient and Tissue Selection

Tumor tissue of histologically proven primary HNSCC diagnosed from 06/2014 to 01/2021 were selected from the archival database of the Department of Pathology and clinical data were obtained from patients' archives at the clinical database (both SAP®), Rostock University Medical Center. Follow-up data were obtained from the regional Cancer Registries. Patients included from 01/2018 and later were additionally included in our HNSCC biobank [21]. Selection criteria were 1) primary tumor site (oral cavity, oropharynx, hypopharynx, larynx and/ or homologous neck lymph node metastases); 2) tumor size > 1.2 cm; 3) >18 years of age. When suitable, tissue samples from resection specimens were preferred for analysis over biopsy material. Cancers diagnosed before 2017 were classified using the 7<sup>th</sup> edition of the Union for International Cancer Control (UICC) tumor, lymph node, metastasis (TNM) classification and classification of tumors diagnosed later classified according to the 8<sup>th</sup> edition (published in 2017 [22, 23]) using the latest edition of WHO classification. Squamous cell cancers of oropharynx with positivity for p16 diagnosed before 2017 met the criterion of the newly established subtype of "p16 positive oropharynx carcinomas" according to the latest TNM classification. In respect of the clinical impact, these tumors were re-classified resulting in down-staging of the nodal status in five patients (pN2b -> pN1). Patient consent of each sample was available. The institutional ethic committee at the University Hospital Rostock approved the study (A2018-0003; A2022-0120). The study was performed in accordance with the Declaration of Helsinki.

### Immunohistochemistry

Formalin-fixed paraffin-embedded 4 µm tissue slides were used. Antigen retrieval was performed with a high pH buffer (20 min at 97 °C). The following steps were performed in an Autostainer link 48 instrument (Leica Biosystems, Wetzlar, Germany): 5 min of incubation in peroxidase-blocking buffer followed by incubation with primary antibody (anti-p16: 1:100, G175-405, BD Bioscience, San Jose, CA, USA; anti-CMTM6: 1:1000, EPR23015-45, Abcam, Cambridge, UK; anti-DKK1: 1:100, SC06-86, GeneTex, Alton Pkwy Irvine, CA, USA; anti-CD163: 1:100, GHI/61, Invitrogen, Waltham, MA, USA; anti-p53: 1:100, Do-7; anti-cd56: 1:50, NCAM1; anti-CD68: 1:100, D4B9C; anti-PD-L1: 1:100, 22C3; anti-ki67: 1:500, Mib-1; anti-CD8: 1:100, c8/144B; all Dako, Glostrup, Denmark) and 3,3'- diaminobenzidine (DAB) detection using the Dako-kit K8000 according to the manufacturer's instructions. In bone containing specimens, soft decalcification was performed by the use of etylenediaminetetra acetic acid to preserve protein structures. Slides were counterstained with hematoxylin. All stains were done on whole slide sections. Appropriate positive and negative controls were used.

### Microscopic evaluation

Firstly, Hematoxylin- Eosin (HE) stained slides were checked for invasive squamous cell carcinoma and its grading. For the assessment of TILs, per section and location (invasive front, tumor center) five areas with the highest density of TILs were identified in 40 x magnification (4x objective lens, 10x ocular lens) and average count within these hot-spots at 200x magnification (20x objective lens, 10x ocular lens, 0.237 mm<sup>2</sup> per field) defined its final categorization into one of the five ranges (varying between absent/0; minimal/1; low/2; intermediate/3 to high/4; supplementary Figure 1). In small sized samples, the whole tumor area was evaluated. Analogous to this schema, cytoplasmic and/or membranous reactivity of DKK1, CD8, CD68, CD163, and CD56 in TILs were evaluated, whereby minimum and maximum expression per marker within all samples defined the ranges of the five subgroups. DKK1 scoring on tumor cells (TC) was performed semi-quantitatively by the percentage of moderately to strongly positive cells. PD-L1 and CMTM6 expression was scored analogous to the tumor proportion score (TPS: percentage of TC with marker expression compared to all TC), the immune cell score (ICS: proportion of tumor area occupied by PD-L1 expressing TILs), and CPS defined as ratio of all marker positive TC, lymphocytes, macrophages to TC in the corresponding area multiplied by 100 (therefore containing no unit) as described [24]. All scores were calculated within an area showing at least 100 viable tumor cells. Any membranous immunoreactivity (independent of concomitant cytoplasmic/nuclear staining) with at least weak intensity was set positive. All samples were categorized PD-L1 *positive vs. negative* (CPS ≥ 1: positive) and CMTM6 *high vs. low* (CPS ≥ 5: high), respectively. Nuclear Ki67 positivity on TC defined its proliferation index, and nuclear p53 reactivity its p53-status (weak expression: wild type; strong expression > 50% of TC: mutant; absent expression: "null pattern" = deleted). Strong continuous nuclear and cytoplasmic staining in > 60% of TC for p16 ("block staining") was set as HPV-positive. In samples with questionable as well as positive p16-pattern, HPV-status was analyzed molecularly. All histological scores were assessed twice by two independent experienced, board-certified pathologists (ASB, AZ) and in cases of divergent results, the final score was built by an intern slide discussion (mainly affecting samples initially grouped as "intermediate", which were subsequently redefined as low or high).

## HPV-Status by molecular pathology

Human papilloma virus (HPV) testing was done with a commercially available kit (VisionArray HPV Chip 1.0, ZytoVision, Bremerhaven, Germany) and applied according to the manufacturer's instructions.

## Statistics

Statistical evaluation was performed using GraphPad PRISM software, version 8.0.2 (GraphPad, San Diego, USA). Values are either reported individual or as the mean  $\pm$  SD. After proving the assumption of normality, differences between individual groups were calculated using the unpaired Student's t-test. If normality failed, the non-parametric Mann-Whitney U test was applied. Multiple comparisons were done using one way ANOVA on ranks (Tukey's multiple comparisons test) or Kruskal Wallis test (Bonferroni's Multiple Comparison Test). Kaplan Meyer survival curves were analyzed using the log rank (Mantel Cox) test. Correlation analysis was done by applying the Pearson correlation or, in case of non-parametric distribution, the Spearman correlation (two-tailed P value). The criterion for significance was taken to be  $p < 0.05$ .

## Results

### Patient and Tumor Characteristics

The study cohort comprised 129 patients, all diagnosed with primary HNSCC. The clinical pathological characteristics are presented in Table 1. Most cases were localized in the oral cavity and oropharynx ( $n=42$  and  $n=46$ , respectively). 16 patients suffered from hypopharyngeal cancer, 22 had a laryngeal cancer and in 3 cases, regional lymph node metastases were obtained. Approximately half of the patients were smokers (53.1 %,  $\geq 10$  py) and one third without critical alcohol consumption (33.1 %). One third of the tumors (32.7 %) were p16<sup>+</sup>, because of a previous HPV infection. In 11 p16<sup>+</sup> cases, molecular HPV testing could not be done due to poor DNA quality. These cases were classified as "HPV-like-p16<sup>+</sup>" because they were localized in the oropharynx (tonsil), without a patients' history of noxae. One case was finally classified as p16<sup>+</sup>/HPV<sup>-</sup>. The tumors were taken from all stages (T1 – T4), with local or distant metastases in 70% and 40% of cases, respectively. From three patients with availability of tumor material from primary and meta/synchronous metastatic/recurrent disease, the staining results of primary carcinomas were included for the further analysis.

### Intra- and inter-individual heterogeneity of the tumor microenvironment

The tumor microenvironment was first studied by HE-stained whole slide sections to estimate the amount and distribution of tumor-infiltrating leukocytes (TILs) (Figure 1A, B). At the invasion front, the TIL-score was significantly higher compared to the tumor center ( $p < 0.0001$ , Figure 1E, left). Subtype analysis of HPV<sup>pos</sup> and HPV<sup>neg</sup> cases revealed higher infiltration levels in the former, notably in both the invasion front and the tumor center (Figure 1E, middle and right). Then, specific immunological subpopulations (T cells, macrophages, and NK cells) were quantified (Figure 1, 2, and supplementary Figure 2). Numbers of

CD8<sup>+</sup> cytotoxic T cells as well as CD68<sup>+</sup> and CD163<sup>+</sup> macrophages differed significantly between the invasive front and the tumor center (Figure 1F, left and Figure 2E, F, left). CD8<sup>+</sup> T cells were higher in the HPV-associated cases, compared to their HPV-unrelated counterpart ( $p < 0.01$  (invasion front) and  $p < 0.05$  (tumor center), Figure 1F, middle and right). By contrast, macrophages (CD68<sup>+</sup>, CD163<sup>+</sup>) were similar between both subtypes (Figure 2E, F, middle and right). Amounts of CD56<sup>+</sup> NK cells were low and showed a similar pattern in each compartment (supplementary Figure 2A, B, E, G).

Tumors in the hypopharynx had less TILs (HE, CD8<sup>+</sup>), both at the invasion front and the tumor center, respectively ( $p < 0.05$  vs. oropharynx, Figure 1G, H). *Vice versa*, oropharyngeal carcinomas exhibited highest values of TILs and CD8<sup>+</sup> cells at the invasion front. Tumors of the oral cavity and the larynx had comparable TIL values (Figure 1G, H). Numbers of CD68<sup>+</sup> and CD163<sup>+</sup> macrophages differed significantly between different anatomical sites. Here again, hypopharyngeal cancers had the lowest numbers of infiltrating CD68<sup>+</sup> and CD163<sup>+</sup> macrophages in each compartment (CD68:  $p < 0.05$  vs. oral cavity and CD163:  $p < 0.05$  vs. larynx; Figure 2G, H).

### **Impact of HPV-Status, anatomical site, TILs, and CD8<sup>+</sup> T cells on overall survival**

Morphological examinations of HPV<sup>pos</sup> and HPV<sup>neg</sup> cancers revealed characteristic patterns in both subtypes regarding differentiation, p53 staining, and Ki-67 proliferation index (Figure 3A-H). Then, we focused on the prognostic impact of the TME on patients' overall survival (OS) upon initial diagnosis. This analysis revealed a significant survival benefit for patients with HPV-associated HNSCC compared to their HPV-unrelated counterpart ( $p < 0.01$ ; Figure 3I). In the HPV-related cohort, 89% of patients received adjuvant therapy (i.e. Cisplatin, Cetuximab, and/or radiotherapy). In four patients, surgery was done without adjuvant therapy. In this small group, two patients are still alive and two deceased. The latter presented with reduced general state of health (ECOG 2 vs. ECOG 0) at diagnosis and an advanced disease stage. In the HPV-unrelated group, the choice of treatment had a minor influence on OS. Dissecting the impact of the anatomical site revealed the best OS for oral carcinomas and the worst outcome for hypopharyngeal cancer (Figure 3J). Likewise, TILs and CD8<sup>+</sup> T cells were positively associated with OS – independent from treatment (Figure 4). For the TILs, this reached statistical significance (invasion front), and for the CD8<sup>+</sup> T cells, the survival benefit was independent from the location within the tumors (invasion front:  $p < 0.001$ ; center:  $p < 0.01$ , Log-rank).

### **PD-L1 and CMTM6-Status and its prognostic impact**

While PD-L1 is an approved biomarker, we tested whether CMTM6 might have comparable prognostic value (Figures 5 and 6). First, a consensus cut-off was established to determine positivity. All samples were categorized into CMTM6 *high vs. low*, with a CPS  $\geq 5$  defined as high. By applying this cut-off, 76.5% of all samples were CMTM6<sup>high</sup>, which is similar to the PD-L1 positivity in this cohort (CPS  $\geq 1$ : 74.4%). Still, PD-L1 and CMTM6 differed between individual samples (representative images are given in Figure 5C-F, Table 1). Concerning PD-L1, there was a strong correlation for CPS and TPS (Spearman  $r = 0.779$ ,

$p < 0.001$ ) as well as for CPS and ICS (Spearman  $r = 0.851$ ,  $p < 0.001$ ) and for ICS and TPS (Spearman  $r = 0.616$ ,  $p < 0.001$ ). By means of CPS, 74.4% of cases had a value  $\geq 1$  with a median CPS of 5 (Figure 5A and D). Concerning CMTM6, there was a highly significant correlation for CPS and TPS (Spearman  $r = 0.730$ ,  $p < 0.0001$ ), and for CPS and ICS (Spearman  $r = 0.242$ ,  $p < 0.01$ ), but not for ICS and TPS (Spearman  $r = -0.041$ ). By means of CPS, 3.4% expressed a score  $< 1$  and 76.5% expressed a score  $\geq 5$ . Median CPS was 25. Given the higher CMTM6 expression by CPS, cases with a CPS  $\geq 5$  were set positive for further analysis (whereas CPS  $\geq 1$  defined PD-L1 positivity). Considering CPS, there was a significant correlation between PD-L1 and CMTM6 expression (Spearman  $r = 0.217$ ; supplementary Figure 3A) with an analogical staining pattern. All samples with a CMTM6 CPS  $\geq 5$  were PD-L1 positive. For both markers, CPS did not differ significantly between HPV-associated and HPV-unrelated HNSCCs (Figure 5A, B, middle). Likewise, the anatomical site had a minor impact on PD-L1 or CMTM6 positivity (Figure 5A, B, right). An exception was seen for the PD-L1 CPS, which was generally lower in hypopharyngeal cancers compared to the other sites (Figure 5A, right).

Patients exhibiting a PD-L1 CPS  $\geq 1$  as well as the subgroup with CMTM6 CPS  $\geq 5$  had a significant longer OS ( $p < 0.0001$  and  $p < 0.01$ , respectively; Log-rank, Figure 6A, B, E, F). Combination of both markers showed a prolonged survival in the subgroup with PD-L1 expression  $\geq 1$  and synchronous CMTM6 expression  $\geq 5$  ( $p < 0.05$ ; Log-rank, Figure 6C, E, F). The CMTM6<sup>high</sup>/PD-L1<sup>neg</sup> and CMTM6<sup>low</sup>/PD-L1<sup>neg</sup> subgroup showed comparable short OS (median OS: 40 months, Figure 6C, G, H, I, J). The best outcome was seen for patients with PD-L1<sup>pos</sup>/HPV<sup>pos</sup> cancers yielding a 100 % survival rate within the follow-up of  $> 80$  months (Figure 6D). *Vice versa*, patients with PD-L1<sup>neg</sup>/HPV<sup>neg</sup> HNSCCs had the worst outcome (median OS: 39 months). A comparable outcome was seen when CMTM6 was considered (supplementary Figure 3B).

CMTM6 CPS correlated significantly with the number of TILs at the center (Spearman  $r = 0.34$ ,  $p < 0.0001$ ) and PD-L1 CPS with TILs at the invasive front (Spearman  $r = 0.266$ ,  $p < 0.01$ ) and both with CD8<sup>+</sup> T cell Score (Spearman  $r =$  range from 0.22 to 0.34). There were no significant differences of PD-L1 or CMTM6 expression between the HPV<sup>pos</sup> or HPV<sup>neg</sup> cases although the latter tended to be more PD-L1 positive ( $p = 0.07$ ; Fishers-exact test).

Taking CD8<sup>+</sup> T cells as additional predictive biomarker (supplementary Figure 3C), patients with CMTM6<sup>high</sup> tumors and a CD8<sup>+</sup> T cell score  $> 1$  showed the best OS (supplementary Figure 3D).

### **Significance of TAMs, NK cells, and DKK1 expression**

Neither the amount of CD163<sup>+</sup> and CD68<sup>+</sup> macrophages, nor numbers of CD56<sup>+</sup> NK cells showed any significant influence on OS (Figure 7, supplementary Figure 2). There was a highly significant correlation between CD68<sup>+</sup>- and CD163<sup>+</sup>-TAMs (Spearman  $r > 0.80$  for both locations,  $p < 0.0001$ ) with analogical staining patterns in the examined samples. Twelve patients having a CD68/CD163-ratio  $> 1$  within the tumor center showed a significantly longer OS than the patients without dominant M1-polarized macrophages (Figure 7C). Within the CD56 stained samples, 10% and 5% had a score  $\geq 3$ , respectively in

each compartment. In the DKK1-stained subgroup, by means of our evaluation method, no clinical pathological relevance of DKK1 was identifiable with 71% of samples with DKK1 positivity on tumor cells (Supplementary Figure 2F, H). DKK1 positive carcinomas showed significantly more DKK1 positive cells in the surrounding stroma than DKK1-negative specimens ( $p = 0.0002$ ; Fisher-exact test).

## Discussion

In this study, we identified CMTM6 as a prognostic biomarker for HNSCC patients. CMTM6 is a regulator of PD-L1 expression and has an important role in the tumor microenvironment (TME) *via* expression on both tumor and immune cells. This finding broadens the spectrum of markers with potential relevance for prognosis and therapy decision.

We studied the prognostic impact of the TME, including TILs, CD8<sup>+</sup> T cells, NK cells, macrophages, DKK1, PD-L1, and CMTM6 positivity on primary HNSCCs located in different anatomical sites. The independent prognostic value of TILs on patients' OS is well established [25, 26] and in HNSCC, high counts of CD8<sup>+</sup> lymphocytes are likewise associated with a better outcome [27]. Here, we confirm the positive prognostic effect of TILs and CD8<sup>+</sup> cells. By contrast, NK cells and DKK1, a regulator of the immune response by the *Wnt* pathway, had a minor impact on OS. This finding contradicts previous reports, describing an unfavorable OS in HNSCC dependent on DKK1 expression status [28]. By contrast, CD68<sup>+</sup> M1-polarized macrophages alone and the M1:M2 ratio, i.e. CD68:CD163, were associated with prolonged OS, as described before in other tumor entities [29, 30]. In HNSCC, M2-like polarization is expected to be driven by the Receptor for activated C kinase 1 *via* NF- $\kappa$ B suppression to promote tumor development [31]. A direct correlation between M2-macrophage infiltration and disease stage can be anticipated.

To our knowledge, this is the first study to investigate the PD-L1 and CMTM6 status in combination with the TME by a plain histological approach in HNSCC. We found that HPV<sup>pos</sup> HNSCC harbored more CD8<sup>+</sup> T cells than HPV<sup>neg</sup> cases, which is in concert with recent literature [32]. The HPV-Status made no difference concerning PD-L1 or CMTM6-Status, but patients with either PD-L1<sup>pos</sup> or CMTM6<sup>high</sup> tumors had a comparable good outcome as the HPV<sup>pos</sup>-subgroup independently of HPV-Status. Although the impact of PD-L1 on OS is contrarily reported in the literature [33], we propose the direct association between PD-L1 and a high TIL infiltration as explanation for the positive prognostic impact. For CMTM6, a comparable positive association is likely, as reported lately in triple-negative breast cancer [34].

In our cohort, nine patients with PD-L1<sup>neg</sup>/ CMTM6<sup>high</sup> cancers had a significantly worse OS compared to the PD-L1<sup>pos</sup>/ CMTM6<sup>high</sup> subgroup. In contrast, CPS of PD-L1 and CMTM6 correlated with CD8<sup>+</sup> T cells, and patients with CMTM6<sup>high</sup> tumors and a CD8<sup>+</sup> T cell score >1 showed a superb OS. This highlights the immune-oncological crosstalk between tumor cells and TILs, which is not only mediated by the druggable target PD-L1 but also by CMTM6. Patients whose tumors are positive for CMTM6 might thus be good candidates for ICI treatments. However, more studies for a detailed understanding of this molecule and its molecular regulation are needed before implementing CMTM6 into routine pathological diagnostics. This



will hopefully help to enhance the prognostic value of PD-L1. Also, standardization of the antibody clones, the scoring system, and the cut-off is imperative to yield homogeneous data sets. To date, no consensus on CMTM6 positivity exists, as it is mostly classified as “low” or “high” [35–37]. This leaves a source of great uncertainty for both oncologists and pathologists. We propose a 5% cut-off for positivity on tumor cells and TILs as “high”. The rationale for choosing 5%, instead of 1% like for PD-L1, is the higher overall expression of CMTM6 in HNSCC. In our cohort, this yielded a CMTM6 positivity of 76.5%, which is similar to PD-L1 positivity (74.4%, CPS  $\geq$ 1). By applying this scoring system, CMTM6 was identified as a reliable and clinically relevant prognostic biomarker and its validity increased by adding PD-L1 and CD8<sup>+</sup> T cells to this marker panel.

Lately, a direct association between PD-L1 and CMTM6 was described for triple-negative breast cancer undergoing epithelial-mesenchymal transition (EMT) [38]. Comparable mechanisms were identified in HNSCC [39]. CMTM6 may thus play a role in the acquisition of cancer stem cell-like properties and in the regulation of EMT through the *Wnt*/ $\beta$ -*catenin* pathway, finally driving Cisplatin resistance [40]. This finding is of particular relevance; however, it does not fit the prognostic relevance of PD-L1 and CMTM6 in our study and warrants further investigations. PD-L1/CMTM6 co-localization maintains its surface expression *via* the prevention of lysosome-mediated degradation. In ovarian and colorectal cancer, a comparable favorable prognostic role was found, which was attributable to an “immunologically hot” TME [18, 19]. Such beneficial effects can be expected in HNSCC, and indeed a positive correlation was seen for CMTM6, PD-L1, and CD8<sup>+</sup> T cells – eventually regardless of EMT.

A good biomarker must be easy to detect or quantify in assays that are both affordable and robust. Besides, it should be uniquely expressed within the tumor. Lastly, a biomarker must yield comparable results between preoperative biopsies and –if available– surgical resection specimens. For PD-L1, the applicability as a biomarker in preoperative biopsies was recently confirmed [41, 42]. Adding to this, neoadjuvant immunotherapy with nivolumab alone or in combination with ipilimumab in patients with loco-regional advanced HNSCC is safe and effective [43]. This finding is of clinical relevance, given the fact that many HNSCC patients present at an local-advanced and thus non-resectable stage. Hence, it will be interesting to examine whether accurate CPS determination of PD-L1 and CMTM6 will improve screening for immunotherapy eligibility and finally enhance treatment responses. The finding of a comparably consistent expression pattern in different anatomical sites raises hope for the validity of CMTM6 as a predictive biomarker for HNSCC.

This study was done on a quite homogeneous patient cohort with primarily advanced HNSCC patients, without prior chemotherapy. Confounding factors, such as intratumor heterogeneity in tumors, were addressed by either evaluating the whole tumor area or by scoring different areas within the specimen. Also, the CPS  $\geq$ 1 as cut-off for PD-L1 positivity negates potential differences in staining intensity between fresh and long-term stored samples as a result of a lower antigenicity in the latter [44].

Still, our study has some limitations: Methodologically, scoring of immunohistochemistry including PD-L1, CMTM6, and general TIL assessment were performed using the “classical” way by eyeball, which

incorporates tumor heterogeneity but might not be as reliable as computational pathology. To maintain a high reproducibility of our data, all scores were built twice by two independent experienced pathologists. The complexity of TME evaluation was balanced by the analysis of five, well-chosen areas per sample. With respect to the limited number of cases in our well-documented patient cohort, a validation of the (highly significant) surveillance concerning the prognostic role of PD-L1 and CMTM6 is reasonable. If verified, possible links should be addressed by a mechanistic approach. The mechanistically hypothesized function of CMTM6 in posttranslational PD-L1 stabilization and the empirically observable comparability concerning the staining pattern of both markers in HNSCC emphasizes the need for more precisely assessment *via* co-localization in the membranous tumor compartment, e.g. using double-immunofluorescence, as proposed recently [45].

In conclusion, we found that CMTM6 is a reliable prognostic marker in HNSCC with even more power if co-expressed with PD-L1. Both proteins show a strong correlation regarding their positivity on TILs and tumor cells and with CD8<sup>+</sup> T cells. We, therefore, propose CMTM6 as an additional predictive biomarker for future ICI research.

## **Declarations**

### **Funding**

This study was supported in part by a grant from the university Rostock medical center (FORUN Grant No. 889038) to ASB.

### **Competing Interests**

The authors have no relevant financial or non-financial interests to disclose.

### **Author Contributions**

ASB: performed development of methodology, data acquisition and interpretation of data, writing and revision of the paper; SZ: assisted in data acquisition and critically reviewed the paper; AZ: performed data acquisition and critically reviewed the paper; BS: performed molecular HPV testing and analyzed data; DFS: recruited patients, provided material support and critically reviewed the paper; MK and A-SB: assisted in data acquisition; CM: performed study concept and design, analysis and interpretation of data, and writing and revision of the paper. AE and CJ critically revised the paper. All authors read and approved the final paper.

### **Data Availability**

“The datasets generated during and/or analysed during the current study are available from the corresponding author on reasonable request.”

### **Acknowledgement**

We thank Mrs. Westphal, Mrs. Krause, Mrs. Clasen and Mrs. Höffer for their excellent technical assistance. Additionally, we are grateful to Dr. Heike Zettl and Mrs. Kloeking for providing clinical data from the cancer registry Mecklenburg-Western Pomerania.

### **Ethics Approval**

The institutional ethic committee at the University Hospital Rostock approved the study (A2018-0003; A2022-0120). The study was performed in accordance with the Declaration of Helsinki.

### **Consent to participate**

“Informed consent was obtained from all individual participants included in the study.”

### **Consent to publish**

“Informed consent was obtained from all individual participants included in the study.”

## **References**

1. Economopoulou P, Psyri A (2017) Epidemiology, Risk factors and Pathogenesis of Squamous Cell Tumours. *Head Neck Cancers Essentials Clin* 1–6
2. Lewis JS, Smith MH, Wang X, et al (2022) Human Papillomavirus-Associated Oral Cavity Squamous Cell Carcinoma: An Entity with Distinct Morphologic and Clinical Features. *Head Neck Pathol.* <https://doi.org/10.1007/S12105-022-01467-0>
3. Tawk B, Debus J, Abdollahi A (2022) Evolution of a Paradigm Switch in Diagnosis and Treatment of HPV-Driven Head and Neck Cancer-Striking the Balance Between Toxicity and Cure. *Front Pharmacol* 12:. <https://doi.org/10.3389/FPHAR.2021.753387>
4. McDermott JD, Bowles DW (2019) Epidemiology of Head and Neck Squamous Cell Carcinomas: Impact on Staging and Prevention Strategies. *Curr Treat Options Oncol* 20:1–13. <https://doi.org/10.1007/s11864-019-0650-5>
5. Cohen EEW, Bell RB, Bifulco CB, et al (2019) The Society for Immunotherapy of Cancer consensus statement on immunotherapy for the treatment of squamous cell carcinoma of the head and neck (HNSCC). *J Immunother Cancer* 7:. <https://doi.org/10.1186/s40425-019-0662-5>
6. Saba NF, Blumenschein G, Guigay J, et al (2019) Nivolumab versus investigator’s choice in patients with recurrent or metastatic squamous cell carcinoma of the head and neck: Efficacy and safety in CheckMate 141 by age. *Oral Oncol* 96:7–14. <https://doi.org/10.1016/J.ORALONCOLOGY.2019.06.017>
7. Tai TS, Lin PM, Wu CF, et al (2019) CDK4/6 inhibitor LEE011 is a potential radiation-sensitizer in head and neck squamous cell carcinoma: An in vitro study. *Anticancer Res* 39:713–720. <https://doi.org/10.21873/anticancer.13167>

8. Yagi T, Baba Y, Ishimoto T, et al (2019) PD-L1 Expression, Tumor-infiltrating Lymphocytes, and Clinical Outcome in Patients With Surgically Resected Esophageal Cancer. *Ann Surg* 269:471–478. <https://doi.org/10.1097/SLA.0000000000002616>
9. Hall PE, Lewis R, Syed N, et al (2019) A phase I study of pegylated arginine deiminase (Pegargiminase), cisplatin, and pemetrexed in argininosuccinate synthetase 1-deficient recurrent high-grade glioma. *Clin Cancer Res* 25:2708–2716. <https://doi.org/10.1158/1078-0432.CCR-18-3729>
10. Chen SMY, Popolizio V, Woolaver RA, et al (2022) Differential responses to immune checkpoint inhibitor dictated by pre-existing differential immune profiles in squamous cell carcinomas caused by same initial oncogenic drivers. *J Exp Clin Cancer Res* 41:123. <https://doi.org/10.1186/S13046-022-02337-X>
11. Emancipator K, Huang L, Aurora-Garg D, et al (2020) Comparing programmed death ligand 1 scores for predicting pembrolizumab efficacy in head and neck cancer. *Mod Pathol* 2020 34:532–541. <https://doi.org/10.1038/s41379-020-00710-9>
12. de Ruiter EJ, Mulder FJ, Koomen BM, et al (2021) Comparison of three PD-L1 immunohistochemical assays in head and neck squamous cell carcinoma (HNSCC). *Mod Pathol* 34:1125–1132. <https://doi.org/10.1038/S41379-020-0644-7>
13. de Ruiter EJ, Mulder FJ, Koomen BM, et al (2021) Comparison of three PD-L1 immunohistochemical assays in head and neck squamous cell carcinoma (HNSCC). *Mod Pathol* 34:1125–1132. <https://doi.org/10.1038/S41379-020-0644-7>
14. Ferris RL, Blumenschein G, Fayette J, et al (2016) Nivolumab for Recurrent Squamous-Cell Carcinoma of the Head and Neck. *N Engl J Med* 375:1856–1867. <https://doi.org/10.1056/NEJMOA1602252>
15. Burtneß B, Rischin D, Greil R, et al (2022) Pembrolizumab Alone or With Chemotherapy for Recurrent/Metastatic Head and Neck Squamous Cell Carcinoma in KEYNOTE-048: Subgroup Analysis by Programmed Death Ligand-1 Combined Positive Score. *J Clin Oncol*. <https://doi.org/10.1200/JCO.21.02198>
16. Zhao Y, Zhang M, Pu H, et al (2021) Prognostic Implications of Pan-Cancer CMTM6 Expression and Its Relationship with the Immune Microenvironment. *Front Oncol* 10:. <https://doi.org/10.3389/FONC.2020.585961>
17. Yaseen MM, Abuharfeil NM, Darmani H (2022) CMTM6 as a master regulator of PD-L1. *Cancer Immunol Immunother*. <https://doi.org/10.1007/S00262-022-03171-Y>
18. Yin B, Ding J, Hu H, et al (2022) Overexpressed CMTM6 Improves Prognosis and Associated With Immune Infiltrates of Ovarian Cancer. *Front Mol Biosci* 9:. <https://doi.org/10.3389/FMOLB.2022.769032>
19. Peng QH, Wang CH, Chen HM, et al (2021) CMTM6 and PD-L1 coexpression is associated with an active immune microenvironment and a favorable prognosis in colorectal cancer. *J Immunother cancer* 9:. <https://doi.org/10.1136/JITC-2020-001638>

20. Mohapatra P, Shriwas O, Mohanty S, et al (2021) CMTM6 drives cisplatin resistance by regulating Wnt signaling through the ENO-1/AKT/GSK3 $\beta$  axis. *JCI insight* 6:. <https://doi.org/10.1172/JCI.INSIGHT.143643>
21. D S, T M, N I, et al (2021) Establishment and characterization of patient-derived head and neck cancer models from surgical specimens and endoscopic biopsies. *J Exp Clin Cancer Res* 40:246. <https://doi.org/10.1186/s13046-021-02047-w>
22. TNM-Klassifikation maligner Tumoren Herausgegeben von Christian Wittekind
23. Slootweg PJ, El-Naggar AK (2018) World Health Organization 4th edition of head and neck tumor classification: insight into the consequential modifications. *Virchows Arch* 472:311–313. <https://doi.org/10.1007/S00428-018-2320-6>
24. Paver EC, Cooper WA, Colebatch AJ, et al (2021) Programmed death ligand-1 (PD-L1) as a predictive marker for immunotherapy in solid tumours: a guide to immunohistochemistry implementation and interpretation. *Pathology* 53:141–156. <https://doi.org/10.1016/J.PATHOL.2020.10.007>
25. Noske A, Möbus V, Weber K, et al (2019) Relevance of tumour-infiltrating lymphocytes, PD-1 and PD-L1 in patients with high-risk, nodal-metastasised breast cancer of the German Adjuvant Intergroup Node-positive study. *Eur J Cancer* 114:76–88. <https://doi.org/10.1016/J.EJCA.2019.04.010>
26. Rapoport BL, Nayler S, Mlecnik B, et al (2022) Tumor-Infiltrating Lymphocytes (TILs) in Early Breast Cancer Patients: High CD3 +, CD8 +, and Immunoscore Are Associated with a Pathological Complete Response. *Cancers (Basel)* 14:2525. <https://doi.org/10.3390/CANCERS14102525>
27. de Ruiter EJ, Ooft ML, Devriese LA, Willems SM (2017) The prognostic role of tumor infiltrating T-lymphocytes in squamous cell carcinoma of the head and neck: A systematic review and meta-analysis. *Oncoimmunology* 6:. <https://doi.org/10.1080/2162402X.2017.1356148>
28. Mitsuda J, Tsujikawa T, Yoshimura K, et al (2021) A 14-Marker Multiplexed Imaging Panel for Prognostic Biomarkers and Tumor Heterogeneity in Head and Neck Squamous Cell Carcinoma. *Front Oncol* 11:. <https://doi.org/10.3389/FONC.2021.713561>
29. Väyrynen JP, Haruki K, Lau MC, et al (2021) The Prognostic Role of Macrophage Polarization in the Colorectal Cancer Microenvironment. *Cancer Immunol Res* 9:8–19. <https://doi.org/10.1158/2326-6066.CIR-20-0527>
30. Kumar AT, Knops A, Swendseid B, et al (2019) Prognostic Significance of Tumor-Associated Macrophage Content in Head and Neck Squamous Cell Carcinoma: A Meta-Analysis. *Front Oncol* 9:656. <https://doi.org/10.3389/FONC.2019.00656/BIBTEX>
31. Dan H, Liu S, Liu J, et al (2020) RACK1 promotes cancer progression by increasing the M2/M1 macrophage ratio via the NF- $\kappa$ B pathway in oral squamous cell carcinoma. *Mol Oncol* 14:795–807. <https://doi.org/10.1002/1878-0261.12644>
32. Gurin D, Slavik M, Hermanova M, et al (2020) The tumor immune microenvironment and its implications for clinical outcome in patients with oropharyngeal squamous cell carcinoma. *J Oral Pathol Med* 49:886–896. <https://doi.org/10.1111/JOP.13055>

33. Sanchez-Canteli M, Granda-Díaz R, del Rio-Ibáñez N, et al (2020) PD-L1 expression correlates with tumor-infiltrating lymphocytes and better prognosis in patients with HPV-negative head and neck squamous cell carcinomas. *Cancer Immunol Immunother* 69:2089–2100. <https://doi.org/10.1007/S00262-020-02604-W/TABLES/3>
34. Shi S, Ma H-Y, Sang Y, et al (2022) Expression and Clinical Significance of CMTM6 and PD-L1 in Triple-Negative Breast Cancer. *Biomed Res Int* 2022:1–10. <https://doi.org/10.1155/2022/8118909>
35. Mamessier E, Birnbaum DJ, Finetti P, et al (2018) CMTM6 stabilizes PD-L1 expression and refines its prognostic value in tumors. *Ann Transl Med* 6:17–17. <https://doi.org/10.21037/ATM.2017.11.26>
36. Dai M, Lan T, Li X, Xiao B (2022) High expression of CMTM6 is a risk factor for poor prognosis of gastrointestinal tumors: A meta-analysis. *Asian J Surg*. <https://doi.org/10.1016/J.ASJSUR.2022.05.086>
37. Muranushi R, Araki K, Yokobori T, et al (2021) High membrane expression of CMTM6 in hepatocellular carcinoma is associated with tumor recurrence. *Cancer Sci* 112:3314–3323. <https://doi.org/10.1111/CAS.15004>
38. Xiao M, Duhem C, Chammout A, et al (2022) CMTM6 and CMTM7: New leads for PD-L1 regulation in breast cancer cells undergoing EMT. *J Cell Biochem* 123:1025–1031. <https://doi.org/10.1002/JCB.30273>
39. Chen L, Yang QC, Li YC, et al (2020) Targeting CMTM6 Suppresses Stem Cell-Like Properties and Enhances Antitumor Immunity in Head and Neck Squamous Cell Carcinoma. *Cancer Immunol Res* 8:179–191. <https://doi.org/10.1158/2326-6066.CIR-19-0394>
40. Chen L, Yang QC, Li YC, et al (2020) Targeting CMTM6 Suppresses Stem Cell-Like Properties and Enhances Antitumor Immunity in Head and Neck Squamous Cell Carcinoma. *Cancer Immunol Res* 8:179–191. <https://doi.org/10.1158/2326-6066.CIR-19-0394>
41. Ambrosini-Spaltro A, Limarzi F, Gaudio M, et al (2022) PD-L1 expression in head and neck carcinoma by combined positive score: a comparison among preoperative biopsy, tumor resection, and lymph node metastasis. *Virchows Arch* 481:93–99. <https://doi.org/10.1007/S00428-022-03322-7>
42. Liu Z, Williams M, Stewart J, et al (2022) Evaluation of programmed death ligand 1 expression in cytology to determine eligibility for immune checkpoint inhibitor therapy in patients with head and neck squamous cell carcinoma. *Cancer Cytopathol* 130:110–119. <https://doi.org/10.1002/CNCY.22501>
43. Hart LL, Ferrarotto R, Andric ZG, et al (2021) Myelopreservation with Trilaciclib in Patients Receiving Topotecan for Small Cell Lung Cancer: Results from a Randomized, Double-Blind, Placebo-Controlled Phase II Study. *Adv Ther* 38:350–365. <https://doi.org/10.1007/s12325-020-01538-0>
44. Karpathiou G, Vincent M, Dumollard JM, et al (2022) PD-L1 expression in head and neck cancer tissue specimens decreases with time. *Pathol - Res Pract* 237:154042. <https://doi.org/10.1016/J.PRP.2022.154042>
45. T A, KK S, TW K, et al (2020) Pembrolizumab in Microsatellite-Instability-High Advanced Colorectal Cancer. *N Engl J Med* 383:2207–2218. <https://doi.org/10.1056/NEJMOA2017699>

# Table 1

Table 1: Clinico-pathological characteristics of the HNSCC cohort.

<b>Group characteristics</b>	<b>Σ n = 129</b>
<b>Female n [%]</b>	22 [82.9]
<b>Male n [%]</b>	107 [17.1]
<b>Median age [years ± SD]</b>	64.0 ± 8.2
<b>ECOG performance status</b>	0.8
<b>Noxae</b>	
smoking [>10 py in %]	53.1
alcohol [>1 drink/d in %]	33.1
<b>Localization [n]</b>	
oral cavity	42
oropharynx	46
hypopharynx	16
larynx	22
lymph node	3
<b>p16/HPV status [n = 107/129]</b>	
positive [%]	33.6
HPV type 16/26/16 & 33/33/35/negative/N/A [%]	69.3/2.8/5.6/5.6/2.8/2.8/11.1
negative [%]	66.4
<b>Grading [only p16 negative, n = 101/129]</b>	
G1/G2/G3 [%]	7.9/67.3/24.8
<b>TNM classification</b>	
T1/T2/T3/T4 [%]	10.9/35.9/20.3/32.8
N0/N1/N2/N3 [%]	28.3/18.1/40.9/12.6
M0/M1/M2 [%]	88.1/4.8/7.1
<b>CPS for PD-L1 and CMTM6 [%]</b>	
PD-L1: ≥1	74.4
CMTM6: ≥5	76.5
<b>Treatment [n = 109/129]</b>	
RT / RCT / RIT	26 / 21 / 6
CTX / ICI	55 / 1



Values are given as absolute/relative numbers and mean  $\pm$  SD. Abbreviations: ECOG - Eastern Cooperative Oncology Group; py pack years; d – day; HPV – human papilloma virus; G1/2/3 grading; CPS – combined positive score; RCT – radio-chemotherapy; RIT – radio-immunotherapy; RT – radiotherapy; CTX – chemotherapy (not specified); ICI – immune-checkpoint inhibition (Nivolumab).

## Figures

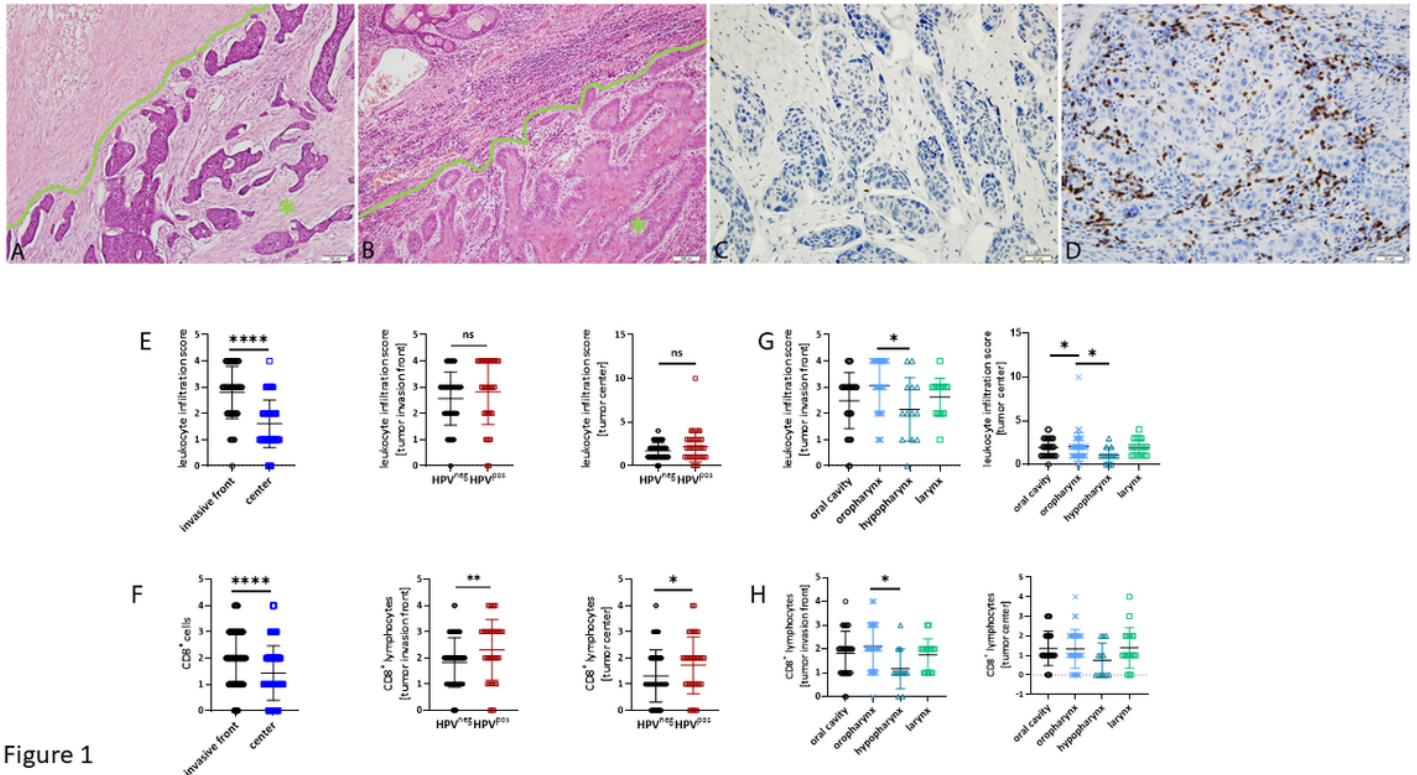


Figure 1

## Figure 1

**Assessment of leukocyte infiltration score by morphology and CD8<sup>+</sup> T cells by immunohistochemistry for the invasive front and the tumor center.** (A-D) Representative slides showing different infiltration patterns in individual tumors with absent (A) leukocyte infiltration (= Score 0; HE, 100x), moderate (B) leukocyte infiltration (= Score 3; HE, 100x), minimal (C) CD8<sup>+</sup> cells (= Score 1, 200x) and high (D) CD8<sup>+</sup> cells (= Score 4, 200x). Asterix = tumor center, green line = invasive front. (E) TILs at the invasive front and the tumor center (left, n=63 invasive front; n=66 center; \*\*\*\*p<0.0001, Unpaired t-test (two-tailed)), as well as between HPV<sup>neg</sup> and HPV<sup>pos</sup> HNSCCs (n=88 HPV<sup>neg</sup>; n=36 HPV<sup>pos</sup>, ns – not significant). (F) CD8<sup>+</sup> cells at the invasive front (left; \*p<0.05, one-way ANOVA (Tukey's multiple comparisons test)) and the tumor center (right; \*p<0.05, one-way ANOVA (Tukey's multiple comparisons test)), as well as between HPV<sup>neg</sup> and HPV<sup>pos</sup> HNSCCs (n=88 HPV<sup>neg</sup>; n=36 HPV<sup>pos</sup>, ns – not significant) (G, H) TILs and CD8<sup>+</sup> cells in

different anatomical sites. n=35 oral cavity; n=36 oropharynx; n=13 hypopharynx; n=16 larynx; \*p<0.05, one-way ANOVA (Tukey's multiple comparisons test))

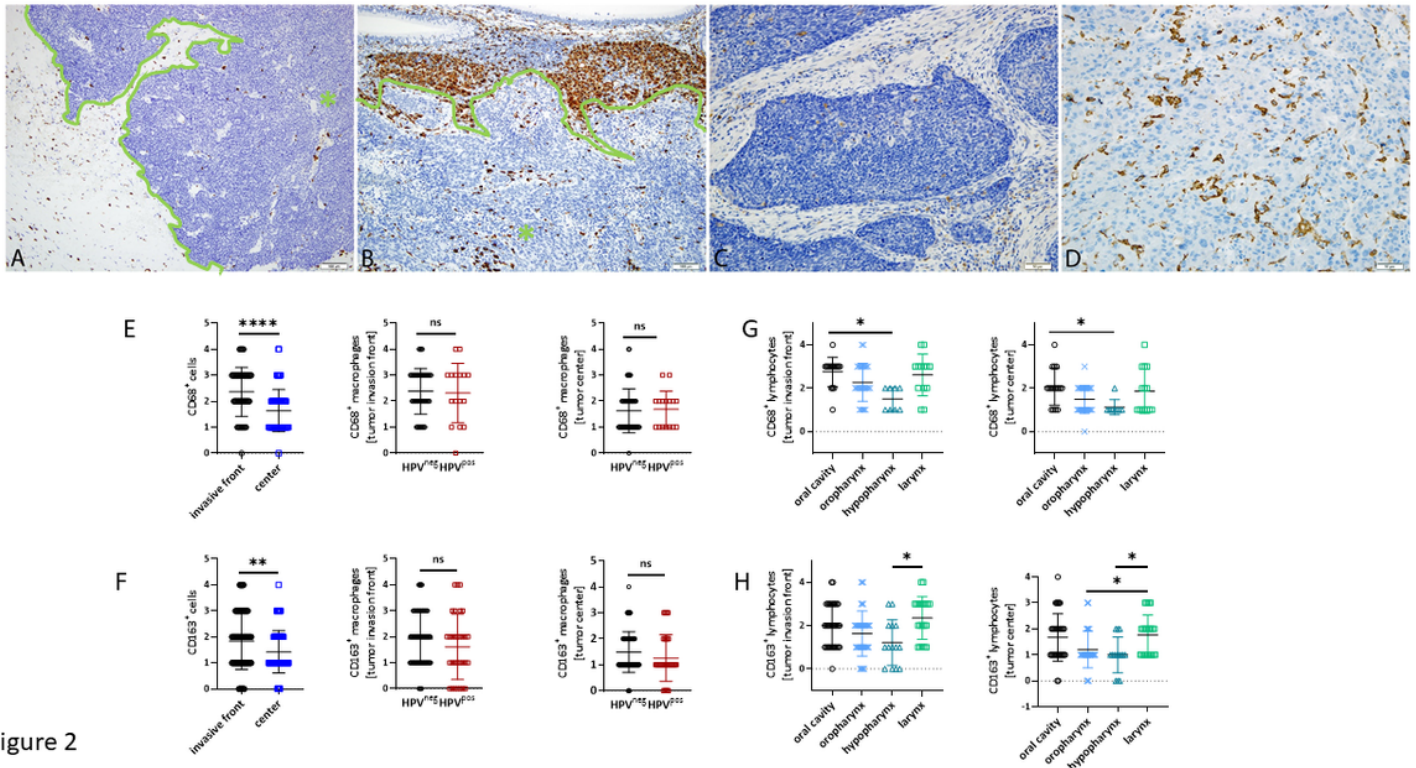


Figure 2

## Figure 2

**Assessment of CD68<sup>+</sup> and CD163<sup>+</sup> cells by immunohistochemistry for the invasive front and the tumor center.** (A-D) Representative slides showing macrophage infiltration patterns (CD68<sup>+</sup>, CD163<sup>+</sup>) in individual tumors with minimal (A) CD68<sup>+</sup> TAMs (= Score 1; 100x), high (B) CD68<sup>+</sup> TAMs (= Score 4; 100x), minimal (C) CD163<sup>+</sup> TAMs (= Score 1, 200x) and high (D) CD163<sup>+</sup> TAMs (= Score 4, 200x). Asterix = tumor center, green line = invasive front. (E) CD68<sup>+</sup> macrophages at the invasive front and the tumor center (left, n=66 invasive front; n=68 center; \*\*\*\*p<0.0001, U-test (two-tailed)), as well as between HPV<sup>neg</sup> and HPV<sup>pos</sup> HNSCCs (n=52 HPV<sup>neg</sup>; n=16 HPV<sup>pos</sup>, ns – not significant). (F) CD163<sup>+</sup> macrophages at the invasive front and the tumor center (left, n=63 invasive front; n=66 center; \*\*p<0.01, U-test (two-tailed)), as well as between HPV<sup>neg</sup> and HPV<sup>pos</sup> HNSCCs (n=84 HPV<sup>neg</sup>; n=31 HPV<sup>pos</sup>, ns – not significant). (G) CD68<sup>+</sup> and (H) CD163<sup>+</sup> macrophages at the invasive front (left; \*p<0.05, Kruskal Wallis test (Dunn's multiple comparisons test)) and the tumor center (right; \*p<0.05, one-way ANOVA (Tukey's multiple comparisons test)) in different anatomical sites. CD68: n=16 oral cavity; n=27 oropharynx; n=8 hypopharynx; n=14 larynx; CD163: n=34 oral cavity; n=41 oropharynx; n=14 hypopharynx; n=20 larynx.

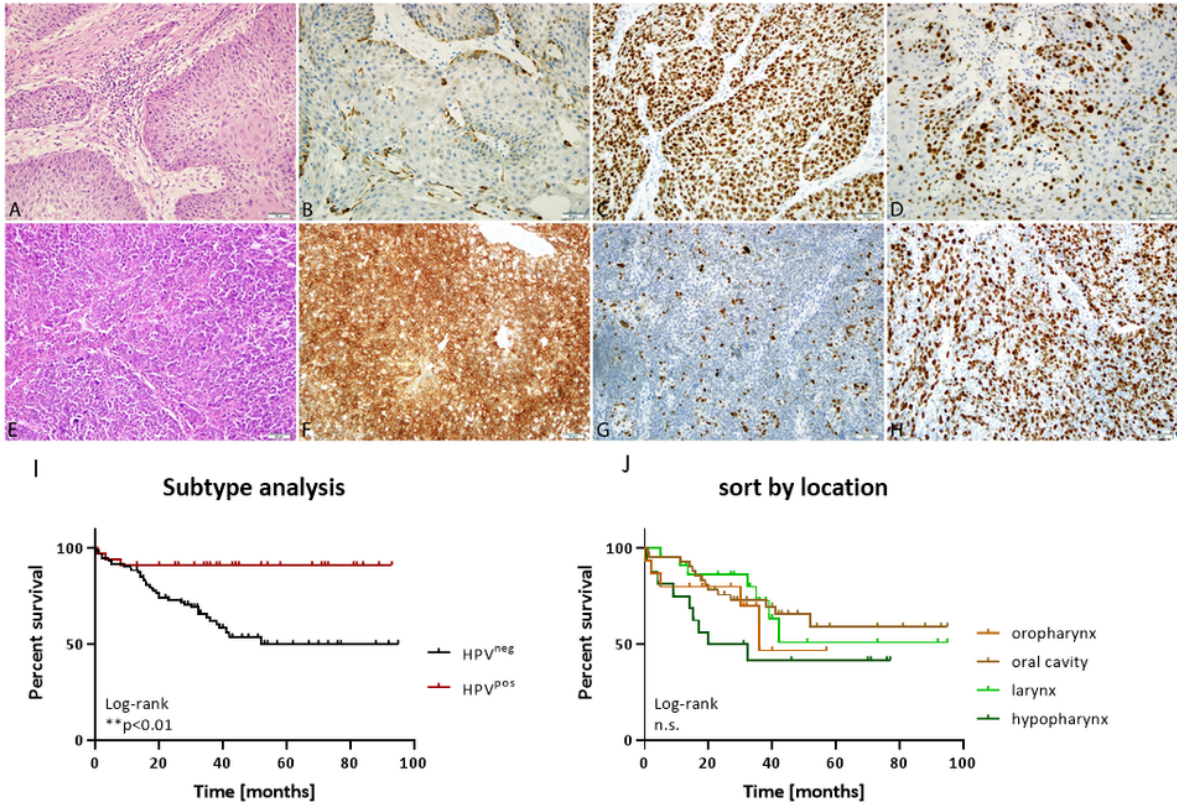


Figure 3

### Figure 3

**Morphology, immunophenotyping and prognostic impact of HPV-negative and HPV-positive cancer.** (A) moderate differentiated squamous cell carcinoma of the larynx (HE staining), p16<sup>INK4A</sup>-negative (B), p53-mutant (C) with moderate proliferation index (D). (E) Poorly differentiated squamous cell carcinoma of the right tonsil, (F) p16<sup>INK4A</sup>-positive with diffuse nuclear and cytoplasmic staining, (G) p53 wildtype and (H) higher proliferation index (200 x magnification). (I) Kaplan-Meier curves show a significant longer OS for HPV<sup>+</sup> cases, n=129; \*\* p<0.01 Log-rank analysis. (J) Kaplan Meier survival curve of HNSCC patients depending on anatomical location revealed best OS for tumors located in the oral cavity; n=126; Log-rank analysis, n.s. – not significant.

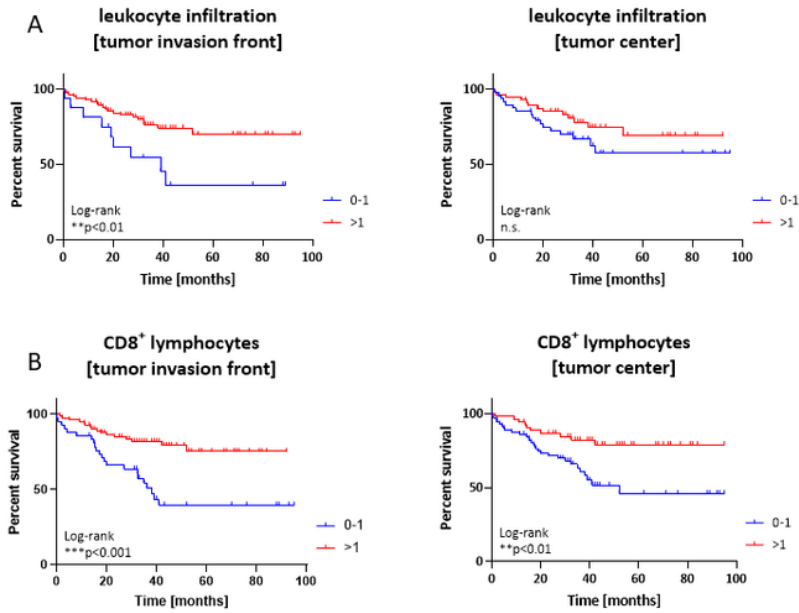


Figure 4

## Figure 4

**Impact of TILs and CD8<sup>+</sup> T cells on overall survival of HNSCC patients.** (A) Prognostic relevance of TILs depending on the location, i.e. tumor invasion front or tumor center. Categorization: 0-1; >1; n=100; \*\* p<0.01 Log-rank analysis. (B) Prognostic relevance of CD8<sup>+</sup> cytotoxic T cells depending on the location, i.e. tumor invasion front or tumor center. Categorization: 0-1; >1; n=100; \*\* p<0.01; \*\*\*p<0.001, Log-rank analysis.

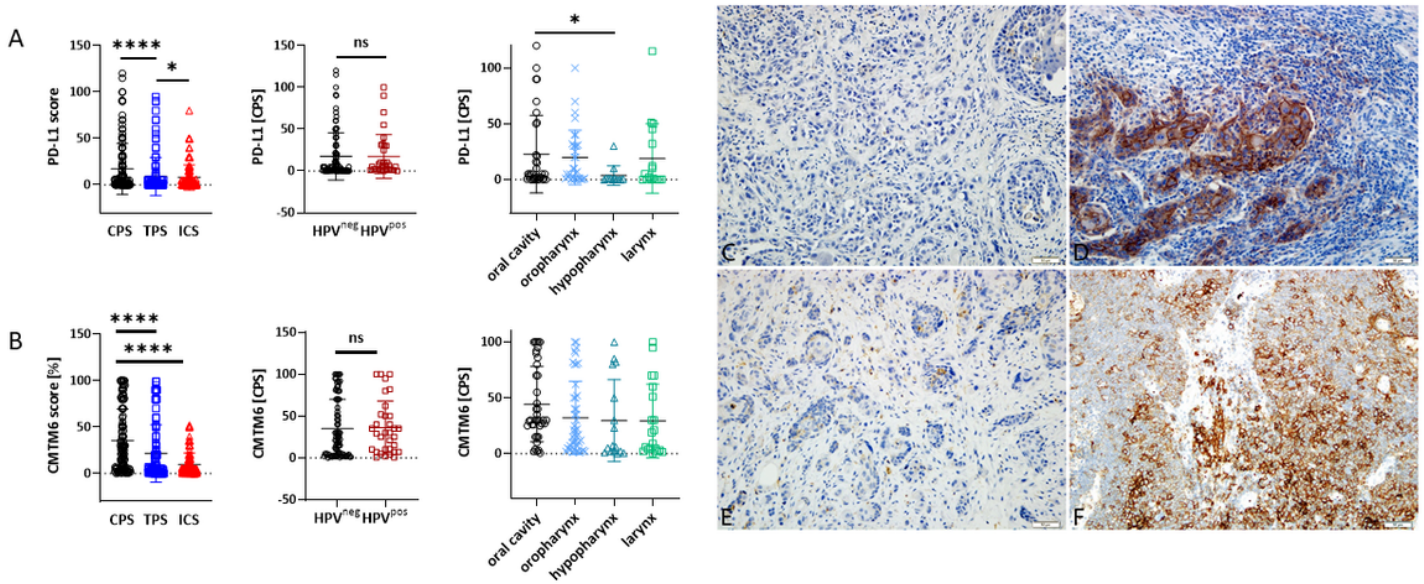


Figure 5

## Figure 5

**Combined Positive Score, Tumor Proportion Score and Immune Cell Score for PD-L1 and CMTM6.** (A) Overall PD-L1 score (CPS, TPS, ICS), and CPS in HPV<sup>neg</sup> and HPV<sup>pos</sup> as well as in different anatomical sites. n=125; \*p<0.05; \*\*\*\*p<0.0001 Kruskal Wallis test (Dunn's multiple comparisons test), ns – not significant). (B) Overall CMTM6 score (CPS, TPS, ICS), and CPS in HPV<sup>neg</sup> and HPV<sup>pos</sup> as well as in different anatomical sites. n=119; \*\*\*\*p<0.0001 Kruskal Wallis test (Dunn's multiple comparisons test), ns – not significant). (C) Squamous cell cancer specimen with negativity for PD-L1 on the tumor cells showing one positive tumor infiltrating lymphocyte (= PD-L1 negative), (D) membranous positivity for PD-L1 on the tumor cells and abundant positive tumor infiltrating lymphocytes (= PD-L1 positive), (E) negativity for CMTM6 on the tumor cells and few positive tumor infiltrating lymphocytes (= CMTM6 low), (F) membranous positivity for CMTM6 on the tumor cells and abundant positive tumor infiltrating lymphocytes (= CMTM6 high; all 200x). For PD-L1, CPS ≥ 1 was set positive, for CMTM6, CPS ≥ 5 was set positive. CPS, Combined Positive Score; TPS, Tumor Proportion Score; ICS, Immune Cell Score.

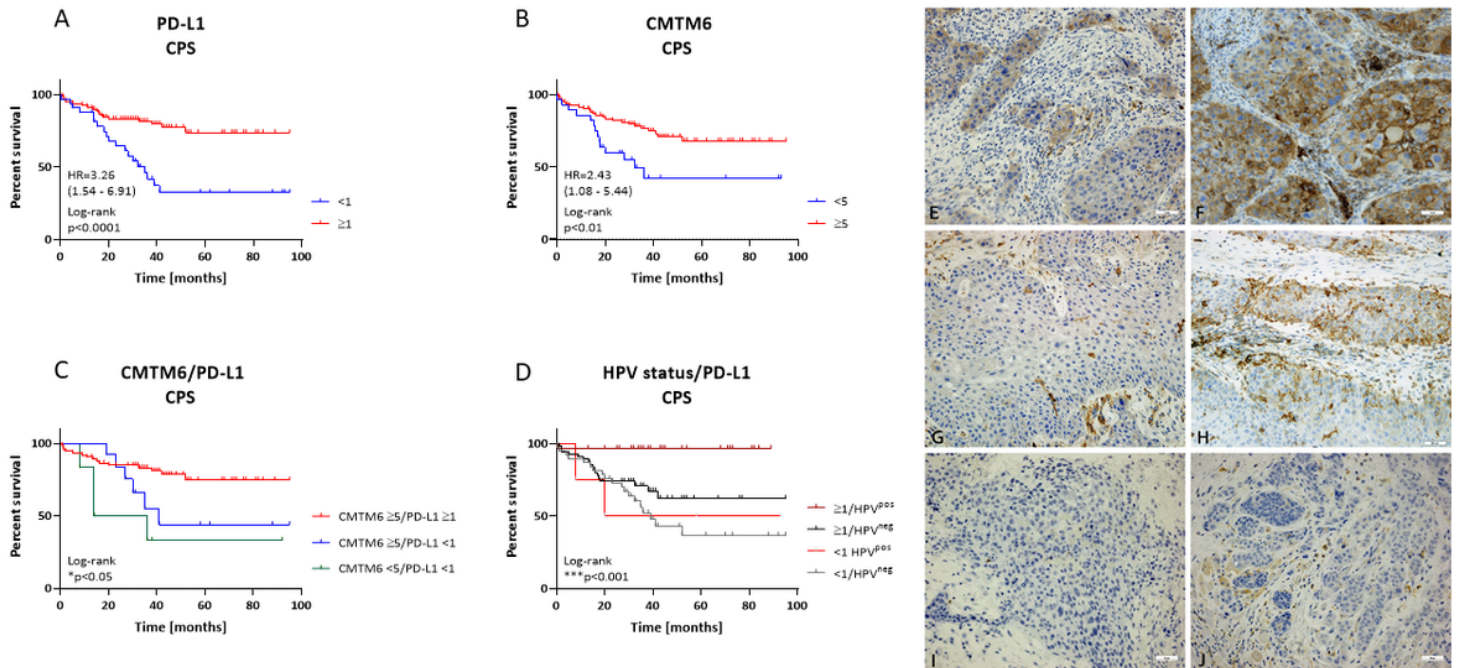


Figure 6

## Figure 6

**Impact of PD-L1 and CMTM6 on overall survival of HNSCC patients.** (A, B) Prognostic relevance of PD-L1 and CMTM6 within HPV<sup>neg</sup> and HPV<sup>pos</sup> cases. CPS: ratio of all marker positive TC, lymphocytes, macrophages to TC in the corresponding area multiplied by 100 (therefore containing no unit). n=128; \*\* p<0.01; \*\*\*p<0.001 Log-rank analysis. (C) Prognostic relevance of PD-L1 and CMTM6 within HPV<sup>neg</sup> and HPV<sup>pos</sup> cases depending on the CPS. n=128; \* p<0.05 Log-rank analysis. (D) Prognostic relevance of PD-L1 CPS according to HPV status. n=128; \*\*\* p<0.001 Log-rank analysis. (E-J) Immunohistochemistry. Paired Examples of cases being PD-L1-positive (E)/ CMTM6 high (F), PD-L1-negative (G, here with positive stained TILs to show reactivity)/CMTM6 high (H) and PD-L1- negative (I)/ CMTM6 low (J). There were no tumors with high PD-L1 but low CMTM6-status.

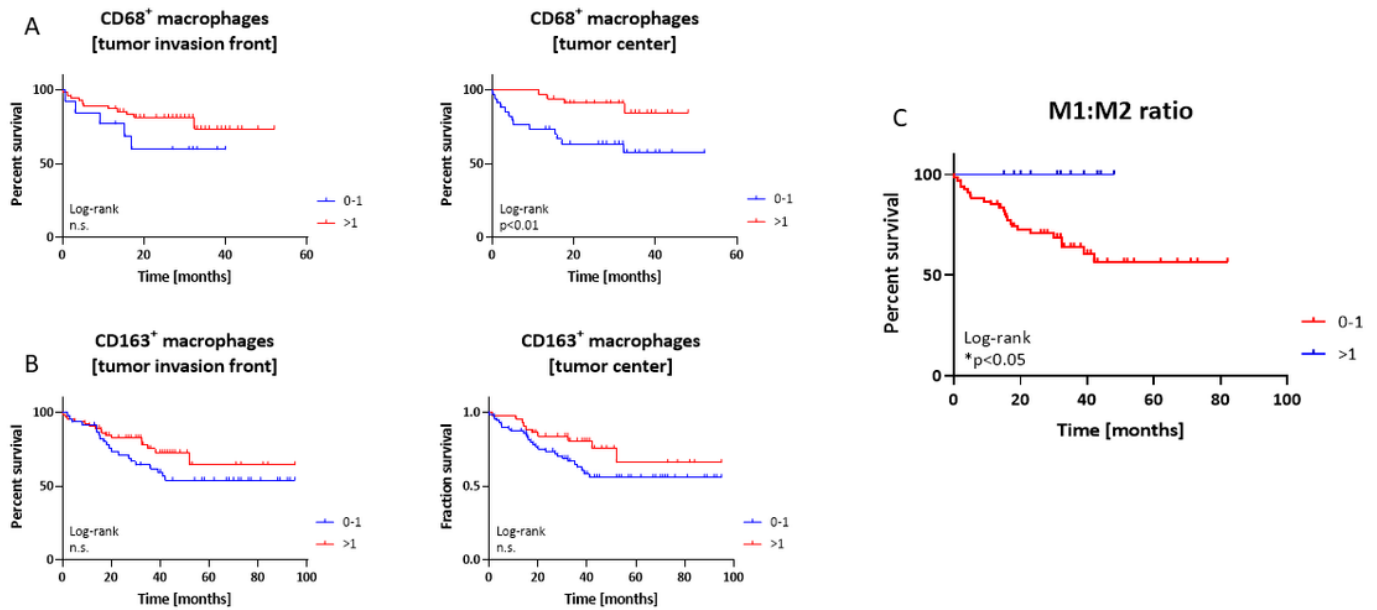


Figure 7

## Figure 7

**Impact of macrophages on overall survival of HNSCC patients.** Prognostic relevance of (A) CD68<sup>+</sup> and (B) CD163<sup>+</sup> TAMs depending on the location, i.e. tumor invasion front or tumor center. Categorization: 0-1; >1; n=100; \*\* p<0.01 Log-rank analysis. Categorization: 0-1; >1; CD68: n=68; CD163: n=112; \*\* p<0.01, Log-rank analysis. (C) The M1:M2 macrophage ratio was calculated by dividing the score of CD68<sup>+</sup> M1 macrophages by the score of CD163<sup>+</sup> M2 macrophages. Categorization: 0-1 n=67; >1; n=12; \* p<0.05, Log-rank analysis.

## Supplementary Files

This is a list of supplementary files associated with this preprint. Click to download.

- [Folie8.tif](#)
- [Folie9.tif](#)
- [Folie10.tif](#)